Molecular Dynamics Simulation Reveals the Selective Binding of Human Leukocyte Antigen Alleles Associated with Behçet's Disease

Sirilak Kongkaew[1], Pathumwadee Yotmanee[2], Thanyada Rungrotmongkol[3,4], Nopporn Kaiyawet[5], Arthitaya Meeprasert[3], Toshikatsu Kaburaki[6], Hiroshi Noguchi[7], Fujio Takeuchi[8], Nawee Kungwan[9], Supot Hannongbua[5]*

1 Program in Biotechnology, Faculty of Science, Chulalongkorn University, Bangkok, Thailand, 2 Department of Chemistry, Faculty of Science, Ramkhamhaeng University, Bangkok, Thailand, 3 Department of Biochemistry, Faculty of Science, Chulalongkorn University, Bangkok, Thailand, 4 Ph.D. Program in Bioinformatics and Computational Biology, Faculty of Science, Chulalongkorn University, Bangkok, Thailand, 5 Computational Chemistry Unit Cell, Department of Chemistry, Faculty of Science, Chulalongkorn University, Bangkok, Thailand, 6 Department of Ophthalmology, University of Tokyo, Tokyo, Japan, 7 School of Pharmaceutical Sciences, University of Shizuoka, Shizuoka, Japan, 8 Department of Internal Medicine, Faculty of Medicine, University of Tokyo, Tokyo, Japan, 9 Department of Chemistry, Faculty of Science, Chiang Mai University, Chiang Mai, Thailand

* Supot.h@chula.ac.th

Abstract

Behçet's disease (BD), a multi-organ inflammatory disorder, is associated with the presence of the human leukocyte antigen (HLA) HLA-B*51 allele in many ethnic groups. The possible antigen involvement of the major histocompatibility complex class I chain related gene A transmembrane (MICA-TM) nonapeptide (AAAAAIFVI) has been reported in BD symptomatic patients. This peptide has also been detected in HLA-A*26:01 positive patients. To investigate the link of BD with these two specific HLA alleles, molecular dynamics (MD) simulations were applied on the MICA-TM nonapeptide binding to the two BD-associated HLA alleles in comparison with the two non-BD-associated HLA alleles (B*35:01 and A*11:01). The MD simulations were applied on the four HLA/MICA-TM peptide complexes in aqueous solution. As a result, stabilization for the incoming MICA-TM was found to be predominantly contributed from van der Waals interactions. The P2/P3 residue close to the N-terminal and the P9 residue at the C-terminal of the MICA-TM nonapeptide served as the anchor for the peptide accommodated at the binding groove of the BD associated HLAs. The MM/PBSA free energy calculation predicted a stronger binding of the HLA/peptide complexes for the BD-associated HLA alleles than for the non-BD-associated ones, with a ranked binding strength of B*51:01 > B*35:01 and A*26:01 > A*11:01. Thus, the HLAs associated with BD pathogenesis expose the binding efficiency with the MICA-TM nonapeptide tighter than the non-associated HLA alleles. In addition, the residues 70, 73, 99, 146, 147 and 159 of the two BD-associated HLAs provided the conserved interaction for the MICA-TM peptide binding.

Introduction

Behçet's disease (BD) has caused recurrent inflammation of symptom complex in genital and oral ulceration, inflammatory lesion of central nervous systems, gastrointestinal tract and eyes leading to blindness [1]. This disease is usually reported in adults aged between 18 to 40 year-olds and presents a higher mortality risk in males than females [2]. A high epidemiology of BD is commonly found in Japan, Turkey, China and the Middle East and the Mediterranean countries [3]. The systemic inflammatory disease is characterized by recurrent exacerbations and spontaneous remissions with varying healing times among patients, and the disease course usually becomes several years or more. On the ocular disease, recurrent and often bilateral episodes of acute exacerbations of intraocular inflammation (ocular attacks) in the anterior chamber (iridocyclitis) normally occur with or without posterior involvement (retinal vasculitis, hemorrhages, exudates, retinal vein occlusion and optic neuritis). Recurrent ocular attacks of posterior involvement lead to poor visual prognosis [4]. Intestinal and neurological diseases are serious complications of BD and can severely deteriorate the patients' psychosomatic status. Because BD can induce severe damage in the eyes and other organs, it is important to clarify the pathogenesis of this disease and to develop a novel treatment based on the pathogenesis.

The exact etiology of this disease has not been clarified yet, but it is probably mediated by a combination of excessive immune reactions, genetics factors [5], immune reactions against infectious agents [6], heat shock proteins [7], oxidative stress [8] and environmental factors. Indeed, several inflammatory cytokines involved in acute inflammatory reactions, such as interleukin (IL)-6, tumor necrosis factor-α and IL-8 might play a role in the pathogenesis of this disease [9]. In addition, genetic factors, including the human leukocyte antigen (HLA)-B51 alleles and especially the HLA-B*51:01 allele is strongly associated with BD across different susceptible ethnic groups [10, 11]. Recently, a meta-analysis of 78 studies involving 4,800 cases of BD and 16,289 controls reported the pooled odds ratio (OR) of HLA B51/B5 carriers to develop BD compared to non-carriers (OR = 5.78 95%, CI = 5.00–6.67) [12].

The notion of an environmental trigger of BD in patients with genetic susceptibilities has long been advocated. Several infectious agents have been investigated, especially bacteria (*Streptococcus*, *Mycoplasma* and *Helicobacter pylori*) and viruses (Herpes simplex virus 1 and 2, Hepatitis virus and Parvovirus B19) [13]. The autoimmunity against bacterial and human heat-shock proteins (HSP) was also speculated as a trigger for BD, because autoantibodies against HSP65 and HSP60 have been reported in BD patients [14].

On the other hand, the genetic association of the major histocompatibility complex (MHC) class I chain related to gene A (MICA) with BD has been reported in various ethnic groups [15, 16], and a strong association of the polymorphism in the transmembrane region of MICA (MICA*009) with BD was observed [17, 18]. The self nonapeptide of AAAAAIFVI located on the MICA transmembrane region (MICA-TM), induced autoreactive CD8+ cytotoxic T lymphocytes in BD patients with HLA-B*51 [19]. Accordingly, the MICA-TM peptide is one of the candidate bechetogenic epitopes [17, 19], where the self-antigen AAAAAIFVI could function as the antigen that triggers the T-cell receptor and develops to an autoimmune reaction [19–21]. The MICA is usually expressed in fibroblasts, monocytes, epithelial cells and endothelial cells in a stress-dependent manner, and plays a key role in initiating the antibody-dependent rejection of organ-transplants [22–24].

The HLA molecules are human equivalents of the MHC found in most vertebrates [25]. They are controlled by genes located at the terminal region at band p21.3 on the chromosome 6. Normally, the HLA molecules play a key role as a guard to protect cells in immune recognition. The HLAs are categorized into three different classes (I, II and II), with HLA class I further divided into three main genes(HLA-A,-B and-C) [26]. The HLA alleles associated with
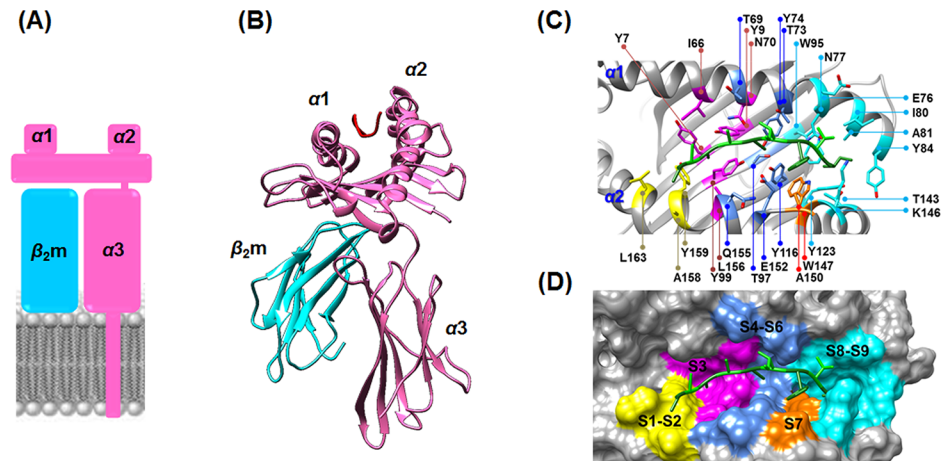
Fig 1. Structural basis of HLA class I. (A) Schematic model of HLA buried in the transmembrane. (B) HLA (pink) contains the α1 and α2 subdomains that contribute to the peptide binding groove, while α3 is the C-terminal domain in complex with ß₂-microgluobulin (ß₂m) as a noncovalently supported protein (cyan). (C) Ribbon and (D) van der Waals surface representations of the MICA-TM nonapeptide (green stick model) occupied in the peptide binding sub-sites (S1–S9, shaded by different colors) of HLA-B*51:01.

BD involve the HLA class I genes HLA-A and HLA-B that importantly function to bind and send short foreign antigens from within the cell to the T-cell receptor (TCR) of CD8+ glycoprotein cells (cytotoxic or killer T-cells) [27]. A digested antigen peptide consisting of 8–13 amino acid residues in length (most commonly 9 to 10 residues) is specifically bound within the peptide-binding groove located on the HLA surface [28, 29]. The binding groove is constructed from the eight ß-strands and α1 and α2 helixes, while α3 and ß₂-microglobulin (ß₂m) are the floor and non-covalent supported units, respectively, as shown in Fig 1 [28]. The different diversity of residues present in the binding-cleft markedly affects the specific binding to the antigen peptide and pathogenesis. The residues at or close to the two ends of the peptide, P2/P3 and P9 residues for the MICA-TM nonapeptide, generally interact with the binding groove of HLA class I and serve as an anchor, whilst the central peptide oozes up out of the groove for direct interaction with the TCR [30, 31]. However, peptides longer than nine residues and up to 13 residues can be recognized by the HLA class I genes through "the middle-out loop shape form" [30], where the residues at or close to the peptide terminals are well occupied in their sub-sites [29].

The association of BD with the HLA-B*51:01 allele in various ethnic groups in Japan and Korea has been frequently observed [3], while the HLA-A*26:01 allele was detected in BD patients in Greece, Japan and Taiwan [32–34]. Some possible candidate genes for BD have been studied in various HLA-A and-B alleles [35]. Recently, in Japanese uveitis patients, BD was associated with the HLA-A*26:01 allele at a 37.5% phenotype frequency more than the controls, and so HLA-A*26:01 is a possible marker as a susceptible allele for ophthalmic BD in Japanese ethnics [36]. By meta-analysis and positive pathergy tests of the Japanese data, the BD clinical manifestations of uveitis, skin lesions and arthritis, and genital ulcers were found to be significantly associated with the HLA-A*26:01, A*02:07 and A*30:04 alleles, respectively [37]. Currently there is no treatment (e.g. vaccine) against BD based upon the HLA recognition antigens despite the apparent restricted association with specific alleles, since the individual risk factors with HLA are unknown. Therefore, we aimed to investigate the link between BD and two specific HLA alleles associated with BD (HLA-A*26:01 and HLA-B*51:01) in terms of their binding affinity to the MICA-TM peptide using MD simulations, in comparison with two

HLA alleles not associated with BD (HLA-A*11:01 and HLA-B*35:01). The molecular understanding of the specific binding of the MICA-TM peptide with the HLA alleles associated with the disease may be useful for therapeutic vaccine design.

Materials and Methods

Structure preparation

The starting structures of three of the HLA class I alleles were taken from the Protein Data Bank, being entries 1E27 [38] for B*51:01 with the HIV-1 epitope at 2.20 Å, 1X7Q [39] for A*11:01 with the SARS nucleocapsid at 1.45 Å, and 1A9E [40] for B*35:01 with the EVB peptide at 2.5 Å (S1 Table). That for A*26:01 was built from homology modeling using the above A*11:01/SARS nucleocapsid structure as a template and the amino acid sequence of A*26:01 from GenBank (accession no. AAA03720) [41], which has 94.3 and 96.6% amino acid identity and similarity to A*11:01, respectively. The HLA/MICA-TM complexes were constructed by changing the original peptide within the X-ray structure to be consistent with the nine amino acids of the antigenic MICA-TM peptide (AAAAAIFVI) using the align sequence profiles module implemented in the Discovery studio 2.5 (Accelrys, Inc.).

MD simulation

The four studied HLA/MICA-TM complexes were investigated by molecular dynamics (MD) simulations using the AMBER 10 software package [42] with the ff03 force field. The missing atoms were added using the LEaP module [43]. The protonation state of all possible charged residues (arginine, lysine, histidine, aspartate and glutamate) in HLA-allele complexes was assigned at pH 7.0 by PROPKA server [44]. The total charges with negative value of the HLA/MICA-TM complexes were randomly neutralized by Na^+ counterions (2, 1, 1 and 2 ions for the B*51:01, B*35:01, A*26:01 and A*11:01 systems, respectively). Afterwards, the individual complex was solvated by TIP3P [45] water molecules leading to approximately 65,000 atoms in total. The dimensions of the simulation box used for all the systems were $86 \times 90 \times 88$ Å^3. The periodic boundary condition with the NPT ensemble and a simulation time step of 2 fs was used. All energy minimizations and MD simulations were performed using the SANDER module of AMBER 10. All bonds and angles concerned to hydrogen atoms were constrained by algorithm of SHAKE [46]. The long-range electrostatic interactions were treated by particle mesh Ewald method and the non-bonded interactions with a cutoff distance of 12 Å were considered [47]. All MD simulations were run with a 12 Å residue-based cutoff for non-bonded interactions and the particle mesh Ewald method was applied for an adequate treatment of long-range electrostatic interactions [48]. Each system was subjected to the four stages of the restrained MD simulations at 298 K with force constants of 10, 7.5, 5 and 2.5 kcal·mol^{-1}·Å^2 for 500 ps in each stage accordingly. These subsequent steps could allow the peptide to adapt its geometry and orientation from the initial model to fit better within the peptide binding groove. Then, the constraints were completely removed and fully unrestrained MD simulations were performed until 50 ns. The convergences of energies, temperature, and global root mean-square displacement (RMSD) were used to verify the stability of the systems. The MD trajectories were collected every 0.2 ps from the production phase for further analysis.

Results and Discussion

Stability of the HLA/MICA-TM complexes

To study the structural stability of the four MD simulations, the RMSDs for all atoms of the four HLA alleles (B*51:01, B*35:01, A*26:01 and A*11:01 alleles) complexed with the
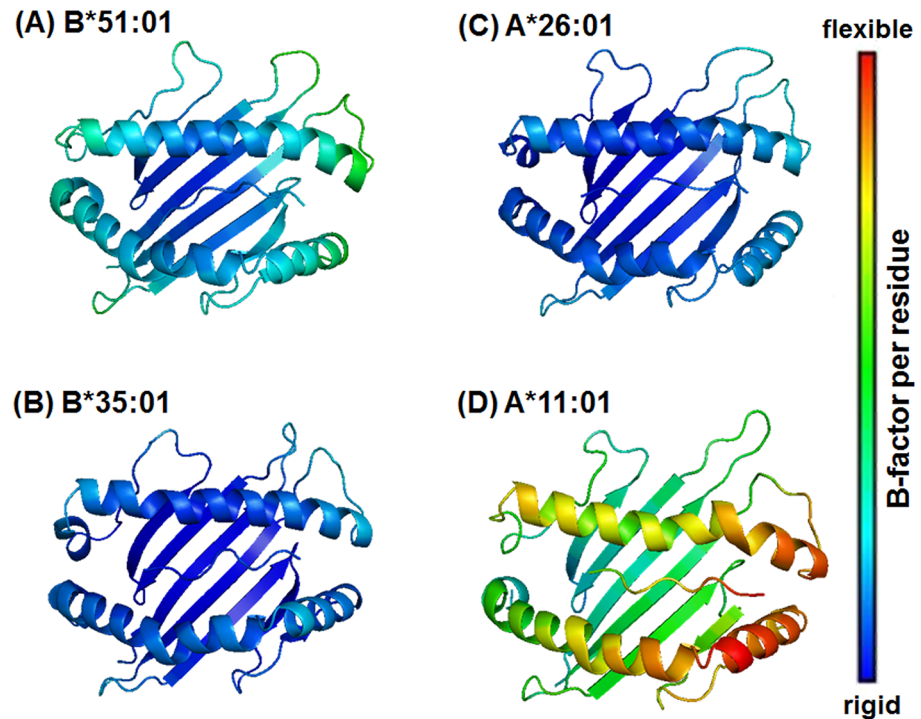
Fig 2. Structural flexibilities of the HLA alleles bound with the MICA-TM peptide. Structural flexibilities were evaluated by B-factor. The ribbon color changes from blue (rigid) to red (flexible) to represent a low to high protein flexibility. Note that for clarity only the binding groove structure and the MICA-TM peptide are shown.

doi:10.1371/journal.pone.0135575.g002

MICA-TM peptide compared with those of the starting structures were monitored along 50 ns of simulation time using the PTRAJ module implemented in AMBER10 package [49]. The RMSD fluctuations of each complex and its structural components (binding groove and β_2-microglobulin) and MICA-TM peptide, were plotted in S1 Fig. The RMSD values quickly increased until ~5 ns and then reached a plateau except for the HLA-B*51:01/MICA-TM complex where the RMSD value continuously increased over the first ~15 ns. The MICA-TM in HLA-B*51:01 system had a low fluctuation around 1 Å, and suddenly at 23 ns, it jumped up to 2 Å until the end simulation. The RMSD increasing caused from the non-polar of MICA-TM peptide change orientation to hydrophobic region within pocket. Although the whole HLA/MICA-TM complex for the two BD-associated HLAs (B*51:01 and A*26:01) fluctuated a great deal, their binding groove and the incoming MICA-TM peptide demonstrated a rather low level of fluctuation. All systems seemed to reach equilibrium after 25 ns with ~1 Å of RMSD fluctuation, and so the MD trajectories from 25 to 50 ns (the production phase) were used for analysis.

Regional flexibility

The backbone flexibility of the HLA-B*51:01, B*35:01, A*26:01 and A*11:01 complexes with MICA-TM were investigated by B-factor calculation over the last 25 ns trajectories (Fig 2). Note that high flexibility of protein was displayed in red and *vice versa* in blue. Among the four systems, the HLA-A*11:01 allele showed the highest degree of protein flexibility in the region of peptide binding groove and in particular at the S7–S9 sub-sites (defined in Fig 1D), whereas the other HLA alleles were likely to have similar degree of flexibility. This might be due to the
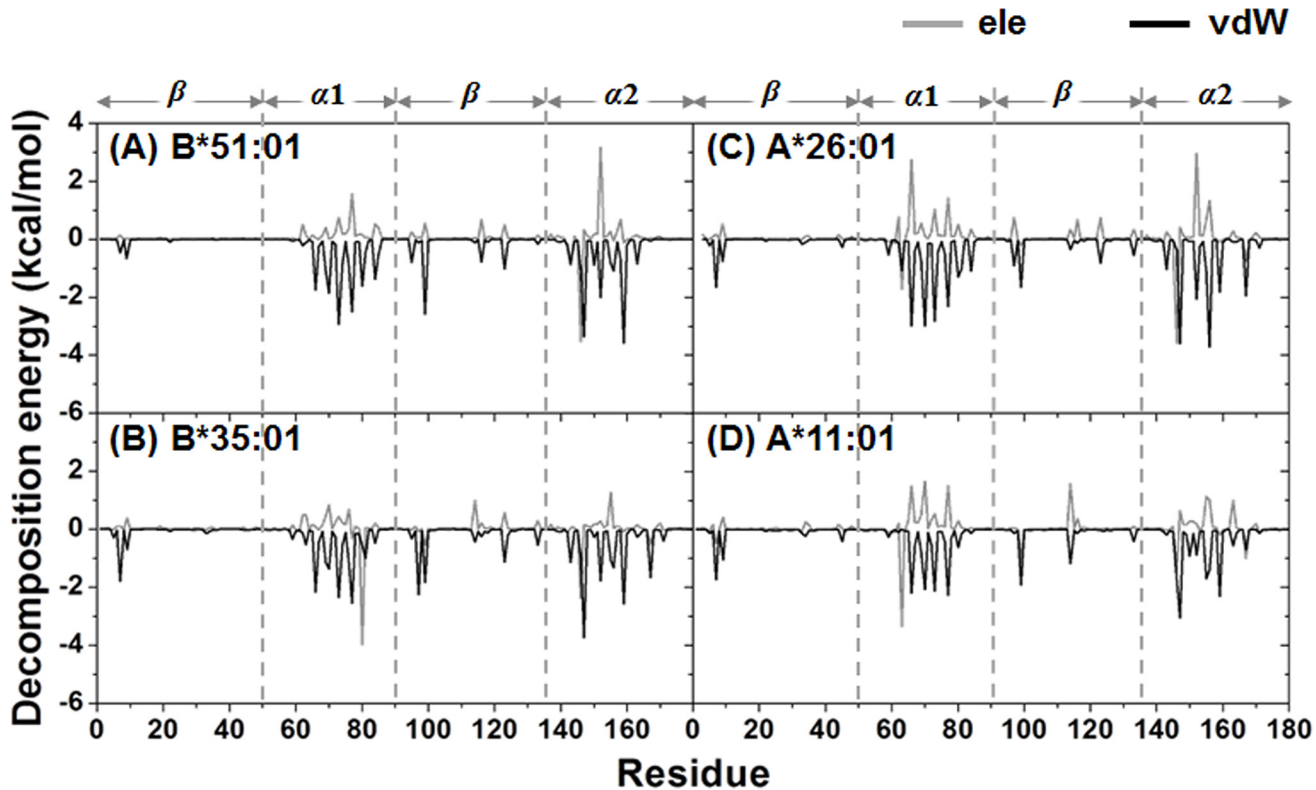
Fig 3. Decomposition energy per HLA residue fingerprint plots. The HLA contribution to the MICA-TM binding is shown in terms of the electrostatic (ele) and van der Waals (vdW) interactions.

strong intramolecular interactions of either the $\alpha 1$ or $\alpha 2$ domains and the intermolecular hydrogen bonds (H-bonds) between the C-terminal of the MICA-TM peptide and the binding residues of the three HLAs (B*51:01, B*35:01 and A*26:01 alleles), which is discussed in a later section.

Per-residue decomposition (DC) energy

The decomposition (DC) energies were calculated and used to scan for potentially important residues for binding [50]. In order to seek the fingerprint of the HLA/MICA-TM interactions, the interaction energy between each HLA residue and the MICA-TM peptide and *vice versa* was calculated over 100 snapshots of the production phase. The obtained DC energies of the HLA and MICA-peptide residues are plotted in Figs [3] and [4], respectively. The HLA/MICA-TM interactions mostly occurred on the $\alpha 1$ and $\alpha 2$ helices with additionally some residues of β-strands ([Fig 3]). Using the criterion of a total DC energy < -0.5 kcal/mol as an important residue, then 22, 18, 16 and 14 potentially important residues of the HLA-B*51:01, B*35:01, A*26:01 and A*11:01 alleles ([S2 Table]), respectively.

Van der Waal (vdW) interactions were found to play an important role in the complex, where the magnitude of the MICA-TM peptide binding with the BD-associated HLA alleles (B*51:01 and A*26:01) was greater than that for the corresponding matched non-BD-associated HLA alleles (B*35:01 and A*11:01). For the nonapeptide, as expected the non-polar residues interacted with HLA through vdW interactions ([Fig 4]). Based on the definition of a total DC energy of < -3 kcal/mol for strong binding, there were four peptide residues that firmly bound to HLA-B*51:01 (P3, P5, P8 and P9) and A*26:01 (P2 and P7–P9), while only two and
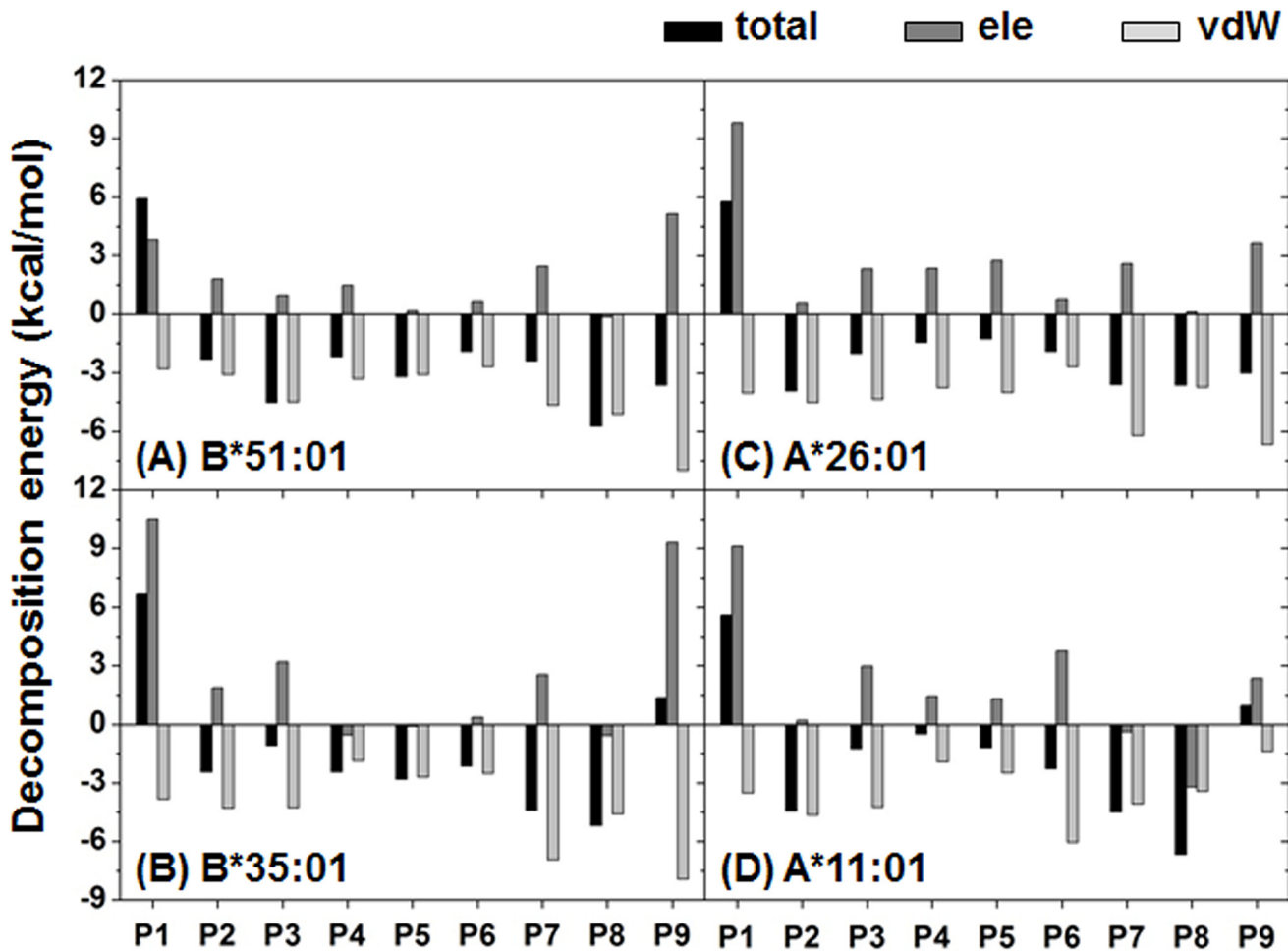
Fig 4. Averaged decomposition energy contributions in HLA binding to MICA-TM. Per-residue decomposition energies and the energy components in terms of the electrostatic (ele) and van der Waals (vdW) interactions for the P1–P9 residues of MICA-TM.

three residues were found in B*35:01 (P7 and P8) and A*11:01 (P2, P7 and P8), respectively. Note that the P9 and P2 or its adjacent residue are known as the anchor for the peptide accommodation at the binding groove of HLA class I [30, 31]. Loss of the P9 contribution may lead to an unbinding recognition of the non-BD-associated HLAs towards the MICA-TM peptide. More details of the interaction and orientation of this peptide at the binding groove of the four HLA alleles investigated are discussed in the hydrogen bond pattern section.

H-bond patterns between HLA and the MICA-TM nonapeptide

To investigate the intermolecular H-bond interactions between the HLA protein and the incoming short MICA-TM nonapeptide, the number of H-bonds was evaluated using the two acceptance criteria of (i) a distance between the proton donor (D) and acceptor (A) atoms of D−A $\leq$ 3.5 Å; and (ii) an angle of D−H···A > 120°, as previously reported [50, 51]. The obtained results were compared between the two paired BD-associated and non-associated HLA alleles in each locus (A or B), and are shown in Fig 5. The peptide binding sub-sites (S1–S9) were classified by the peptide contact position in the binding groove of HLA, as seen in the
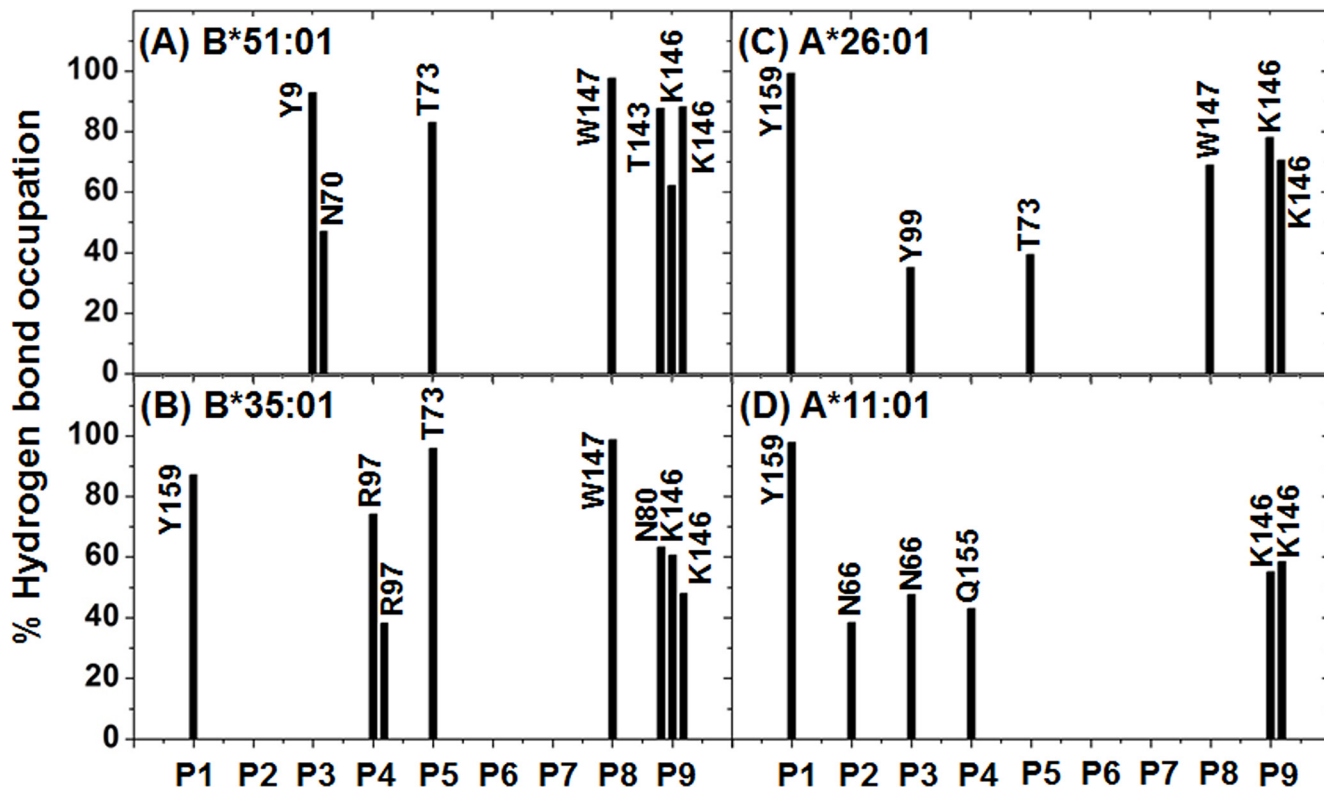
Fig 5. Hydrogen bond interactions. The percentage occupancy of H-bonds averaged over the last 25 ns of simulation time between the nine residues (P1–P9) of the MICA-TM peptide and the HLA residues for the four complexes.

doi:10.1371/journal.pone.0135575.g005

HLA-B*51:01/peptide complex (Fig 1D). The last snapshot of each complex was used to represent the protein-protein H-bond formation detected from the MD simulations (see in S2 Fig).

As shown in Fig 1D, the peptide binding groove of HLA class I is constructed by at least five sub-pockets with a large groove volume (S1 and S2 yellow; S3 magenta; S4–S6 dark blue; S7 orange; S8 and S9 light blue), and it is able to support a variety of incoming short peptides in the binding step. Moreover, the binding groove of the HLA protein provides a hydrophobic cavity to support the nine spanning residues (AAAAAIFVI) of the MICA-TM peptide. Due to the nonpolar nature of this peptide, H-bond formation with the HLA protein was expected through the peptide backbones. In Fig 5A and 5B, both HLA-B alleles similarly stabilized the P9 residue of the MICA-TM peptide by the formation of three H-bonds which two of them are the salt bridge interactions between the C-terminal carboxylate group and the ammonium group of K146. The C-terminal residue (P9) could bind significantly stronger with the BD-associated HLA allele than the non-associated allele (~60–90% H-bond occupation compared to only ~50–70% in the non-associated allele), which could be due to the different residue 80 on the α1 helix (I80 in HLA-B*51:01 and N80 in HLA-B*35:01). Through the strong H-bond (70% occupancy) with the amide group of N80 (Fig 5B), this polar residue at the S9 sub-site of the peptide induced the C-terminal to change its orientation and move closer to the α1 helix of the non-associated BD HLA-B*35:01 (S2 Fig) with the consequence of weakened H-bonds with the α2 helix from the loss of interaction with T143 and a decreased interaction with K146. With respect to the N-terminus of the MICA-TM peptide, the Y159 residue on the α2 helix of the HLA-B*35:01 allele strongly interacted with the P1 residue ($\sim$90%), whilst this end of the

peptide had no interaction with any HLA-B*51:01 residues but instead the P3 residue was stabilized by two α1-helix residues, Y9 and N70, with $\sim$90 and $\sim$50% H-bond occupations, respectively (Fig 5A and S2 Fig). The rearrangement of the H-bonding network at the N-terminal was previously observed in the octamer and nonamer peptides binding to HLA-B*51:01 [38]. In addition to the protein-protein interactions at the two peptide ends, a strong H-bond was formed between the backbone of the P5 Ala residue and the side chain of the T73 residue on α1 helix in the P4–P6 pocket in both HLA-B alleles ($>$ 80%, Fig 5A and 5B). This is congruent with the previous observation that the P5 residue of HIV epitopes (Ile, Val and Pro) was found as an unexpected anchor deeply pointing into the sub-pocket of the binding groove of HLA-B*51:01 [38]. In addition, these two HLA-B alleles had a strong H-bond between the P8 backbone of the MICA-TM nonapeptide and the W147 indole ring on the α2 helix.

In the case of the two HLA-A alleles (Fig 5C and 5D), the N- and C-terminal regions of the MICA-TM peptide showed a firmly established interaction, P1 with the Y159 phenyl ring (~100%) and P9 formed two H-bonds or salt bridge interactions with the K146 ammonium group (~70–80% in the BD-associated HLA-A*26:01, but $<$ 60% in the non-associated one), respectively, at the α2 helix. Only HLA-A*26:01 (Fig 5C) contained a strong interaction at the nearly C-terminal end (P8 residue) with the α2 helix residue W178 (~70%) and the anchor P5 residue weakly interacted with the α1 helix residue T73 (~40%). The Y99 residue on the β-sheet of HLA-A*26:01 somewhat stabilized the P3 residue of MICA-TM (~40%), while the α1 helix residue N66 in HLA-A*11:01 supported the P2 and P3 residues (~40–50%). It is worthy to note that the high protein flexibility of HLA-A*11:01 (Fig 2D) had consequently led to a low binding of the incoming peptide, and in particular at the P5–P9 residues.

Based on the formed H-bonds, the peptide binding recognition was better distinguished in the HLA-A alleles. The lowered binding strength at the C-terminal P9 residue observed in HLA-B*35:01 was suspected to be the most important reason for the low selective binding affinity of this non-BD-associated HLA-B*35:01 allele. Thus, the relatively high protein flexibility in the non-associated HLA-A*11:01 allele led to a decreased H-bond strength with the P9 residue and no stabilization for the P5 and P8 residues. All simulations fairly agreed with the crystal structures of the HLA/peptide complexes in which this P6 residue outwardly located off the binding groove [31].

HLA/peptide binding affinity

To determine the MICA-TM peptide binding strength towards the four studied HLA alleles, the molecular mechanic/Poisson-Boltzmann surface area (MM/PBSA) approach was applied on the same set of 100 snapshots taken from the production phase. The MM/PBSA approach has been extensively used to predict the overall Gibbs free energy (ΔG_{bind}) in biomolecular systems [52]. The ΔG_{bind} of the HLA alleles with the peptide bound at the binding groove was calculated from a summation of the total MM energy (ΔE_{MM}), the solvation free energy (ΔG_{sol}) and the entropic term (TΔS). The last term was estimated from the normal mode analysis [53]. Although the ΔE_{MM} components suggested that the short peptide was better stabilized by the non-BD-associated HLAs in the gas phase, the large destabilization from the solvation effect on the HLA/peptide complex led to a lower total ΔG_{bind}. Rather, within each paired HLA-I gene (HLA-A or HLA-B), the MICA-TM peptide interaction was stronger with the BD-associated allele, where B*51:01 (-56.10 kcal/mol) $>$ B*35:01 (-48.88 kcal/mol) and A*26:01 (-42.97 kcal/mol) $>$ A*11:01 (-31.14 kcal/mol) in Table 1. The obtained results from the present study help to differentiate the HLA alleles and explain a source of BD.

Table 1. The binding free energy and energy components (kcal/mol) for the four HLA/MICA-TM complexes predicted by the MM/PBSA method.

	HLA-B*51:01 [a]	HLA-B*35:01 [b]	HLA-A*26:01 [a]	HLA-A*11:01 [b]
ΔE_{vdW}	-74.7 ± 4.2	-78.1 ± 4.7	-80.0 ± 4.8	-63.7 ± 4.2
ΔE_{elec}	-168.4 ± 16.4	-199.4 ± 17.1	-127.2 ± 20.8	-208.1 ± 25.3
ΔE_{MM}	-243.1 ± 16.1	-277.6 ± 16.4	-207.3 ± 21.6	-271.7 ± 25.0
ΔG_{polar}	199.1 ± 13.9	241.1 ± 14.8	177.3 ± 20.4	252.2 ± 23.6
$\Delta G_{non-polar}$	-12.1 ± 0.4	-12.5 ± 0.3	-13.0 ± 0.3	-11.6 ± 0.4
ΔG_{sol}	187.0 ± 13.9	228.7 ± 14.8	164.3 ± 20.4	240.6 ± 23.4
$-T\Delta S$	9.7±25.8	12.7±24.1	21.5±28.6	15.4±21.4
ΔG_{bind}	-46.4	-36.2	-21.5	-15.7

HLA alleles are

[a] associated or

[b] not associated with Behçet's disease (BD).

Data are shown as the mean ± SD, derived from independent simulations. Means within a paired row (HLA-A or HLA-B alleles that are associated with BD versus that are not) followed by a different letter are significantly different.

ΔG_{bind} is the binding energy with inclusion of entropic term.

doi:10.1371/journal.pone.0135575.t001

Conserved interaction of the BD associated HLAs

Based on MM/PBSA method, the alanine scanning mutagenesis commonly used to signify the important function of residues was carried out on the two BD associated HLA residues within the 5 Å sphere of the MICA-TM peptide. The results of the relative binding free energy ($\Delta\Delta G_{binding} = \Delta G_{wild-type} - \Delta G_{mutant}$) are given in Table 2. Note that the entropy term of the complex is not significantly changed by only one residue substitution with alanine; therefore the entropic calculation was neglected. By a mutation to alanine on the 40 residues, the HLA residue numbers 70, 73, 99, 146, 147 and 159 contributing the $\Delta\Delta G$ value < -2 kcal/mol in either HLA-B*51:01 or HLA-A*26:01 (Table 2) were considered as the important residues. These six residues could provide the conserved interaction of both BD associated HLAs for binding of the incoming MICA-TM.

Conclusions

BD is a multi-organ inflammatory disorder with vasculitis, in which the main cause and mechanism of action are still not well understood. From clinical investigations, the HLA-B*51:01 and HLA-A*26:01 with MICA*009 containing the nonamer peptide (AAAAAIFVI or MICA-TM) are most frequently detected in BD patients. Herein, we aimed to search for the selective correlation between the two BD-associated HLA alleles (HLA-A*26:01 and HLA-B*51:01) and the MICA-TM peptide in comparison with two class matched non-BD-associated HLA alleles (HLA-A*11:01 and HLA-B*35:01) by MD simulations. From the simulations, more contact residues at the binding groove of the BD-associated HLA alleles stabilized the incoming MICA-TM peptide than at the non-associated alleles of the same class (22 and 16 residues for B*51:01 and A*26:01; 18 and 14 residues for B*35:01 and A*11:01). The vdW force was found to be the main protein-protein interaction, but in addition strong H-bonds (>70% occupation) were likely formed with the backbone of the nonpolar peptide, and these were stronger in the BD-associated HLA alleles. The P2/P3 and P9 residues (close to and at the peptide ends, respectively) acted as the anchor for the peptide accommodation at the binding groove of the BD-associated HLAs. The total binding free energy of the HLA/peptide complex suggested a significantly stronger binding strength of the MICA-TM peptide with the

Table 2. Relative binding free energy upon alanine mutation ($\Delta\Delta G_{binding}$) for the HLA residues within 5 Å sphere of the MICA peptide. The residues with $\Delta\Delta G_{binding}$ of < -2 kcal/mol for both HLA classes are shown in bold text.

residue	$\Delta\Delta G_{binding}$ (kcal/mol)	
	HLA-B*51:01	HLA-A*26:01
Y7	-0.43	-2.40
Y9	-1.49	-0.06
I66/N66	-1.89	-1.90
N70/H70	-3.37	-2.57
T73	-2.42	-2.45
Y74/D74	-1.67	-0.94
N77	-1.68	-0.73
I80/T80	-1.31	-0.57
A81/L81	0	-0.93
Y84	-0.53	-1.14
Y85	-1.01	-0.11
W95/I95	-1.04	-0.16
T97/R97	-0.08	-3.42
Y99	-2.52	-2.22
Y116/D116	-0.99	-1.07
Y123	-1.65	-1.19
T143	-2.25	-1.44
K146	-3.68	-2.08
W147	-5.54	-4.64
E152	-1.76	-0.82
Q155	-0.15	-2.12
L156/W156	-1.04	-3.44
Y159	-3.63	-2.85
W167	-0.03	-1.82

doi:10.1371/journal.pone.0135575.t002

BD-associated HLA alleles in the same class (B*51:01 > B*35:01 and A*26:01 > A*11:01). The residues 70, 73, 99, 146, 147 and 159 provided the conserved interaction of the two BD-associated HLAs with the MICA-TM peptide. All the structural, dynamics and energetics information somewhat explain the recognition and selective binding of the MICA-TM peptide towards the specific HLAs related to the BD pathogenesis.

Supporting Information

S1 Fig. Stability of the HLA/MICA-TM complexes. Root-mean square displacements (RMSDs) of all atoms relative to those of the initial structure for the HLA/MICA-TM complex, peptide binding groove, ß$_2$-microglobulin and MICA-TM peptide in the (A) B*51:01, (B) B*35:01, (C) A*26:01 and (D) A*11:01 HLA alleles bound to the MICA-TM peptide. (TIF)

S2 Fig. Hydrogen bond interactions (dashed line) in the HLA/MICA-TM complexes. The MICA-TM peptide and HLA residues at the binding groove are shown in green and white sticks. (TIF)

S1 Table. Crystal structures used for simulation and number of reported BD patients in association and non-association with HLAs.
(DOCX)

S2 Table. HLA residues with a total decomposition (DC) free energy ($\Delta G_{residue}$) of less than -0.5 kcal/mol.
(DOCX)

Acknowledgments

Author Contributions

Conceived and designed the experiments: HN FT TK SH TR SK PY. Performed the experiments: SK PY. Analyzed the data: SK PY TR N. Kaiyawet AM. Contributed reagents/materials/analysis tools: SK PY TR N. Kaiyawet AM SH. Wrote the paper: SK PY TR N. Kaiyawet AM TK HN FT N. Kungwan SH.

References

1. Marshall SE. Behçet's disease. Best Pract Res Clin Rheumatol. 2004; 18(3):291–311. PMID: 15158742

2. Saadoun D, Wechsler B, Desseaux K, Huong DLT, Amoura Z, Resche-Rigon M, et al. Mortality in Behçet's disease. Arthritis Rheum. 2010; 62:2806–12. doi: 10.1002/art.27568 PMID: 20496419

3. Kaya TI. Genetics of Behçet's disease. Patholog Res Int. 2012; 2012.

4. Kaburaki T, Araki F, Takamoto M, Okinaga K, Yoshida A, Numaga J, et al. Best-corrected visual acuity and frequency of ocular attacks during the initial 10 years in patients with Behçet's disease. Graefes Arch Clin Exp Ophthalmol. 2010; 248(5):709–14. doi: 10.1007/s00417-009-1234-z PMID: 19997745

5. Hughes T, Coit P, Adler A, Yilmaz V, Aksu K, Düzgün N, et al. Identification of multiple independent susceptibility loci in the HLA region in Behçet's disease. Nat Genet. 2013; 45(3):319–24. doi: 10.1038/ng.2551 PMID: 23396137

6. Kaneko F, Oyama N, Nishibu A. Streptococcal infection in the pathogenesis of Behçet's disease and clinical effects of minocycline on the disease symptoms. Yonsei Med J. 1997; 38(6):444–54. PMID: 9509915

7. Tanaka T, Yamakawa N, Koike N, Suzuki J, Mizuno F, Usui M. Behçet's disease and antibody titers to various heat-shock protein 60s. Ocul Immunol Inflamm. 1999; 7(2):69–74. PMID: 10420201

8. Chambers JC, Haskard DO, Kooner JS. Vascular endothelial function and oxidative stress mechanisms in patients with Behçet's syndrome. J Am Coll Cardiol. 2001; 37(2):517–20. PMID: 11216972

9. Remmers EF, Cosan F, Kirino Y, Ombrello MJ, Abaci N, Satorius C, et al. Genome-wide association study identifies variants in the MHC class I, IL10, and IL23R-IL12RB2 regions associated with Behçet's disease. Nat Genet. 2010; 42(8):698–702. doi: 10.1038/ng.625 PMID: 20622878

10. Ohno S, Ohguchi M, Hirose S, Matsuda H, Wakisaka A, Aizawa M. Close association of HLA-Bw51 with Behçet's disease. Arch Ophthalmol. 1982; 100(9):1455–8. PMID: 6956266

11. Mizuki N, Inoko H, Ando H, Nakamura S, Kashiwase K, Akaza T, et al. Behçet's disease associated with one of the HLA-B51 subantigens, HLA-B*5101. Am J Ophthalmol. 1993 116(4):406–9. PMID: 8213969

12. Menthon Md, Lavalley MP, Maldini C, Guillevin L, Mahr A. HLA-B51/B5 and the risk of Behçet's disease: a systematic review and meta-analysis of case-control genetic association studies. Arthritis Rheum. 2009; 61(10):1287–96. doi: 10.1002/art.24642 PMID: 19790126

13. Chambrun MPd, Wechsler B, Geri G, Cacoub P, Saadoun D. New insights into the pathogenesis of Behçet's disease. Autoimmun Rev. 2012; 11(10):687–98. doi: 10.1016/j.autrev.2011.11.026 PMID: 22197900

14. Ergun T, Ince U, Ekşioğlu-Demiralp E, Direskeneli H, Gürbüz O, Gürses L, et al. HSP 60 expression in mucocutaneous lesions of Behçet's disease. J Am Acad Dermatol. 2001; 45(6):904–9. PMID: 11712037

15. Mizuki N, Ota M, Katsuyama Y, Yabuki K, Ando H, Goto K, et al. Association analysis between the MIC-A and HLA-B alleles in Japanese patients with Behçet's disease. Arthritis Rheum. 1999; 42 (9):1961–6. PMID: 10513813

16. Mizuki N, Meguro A, Tohnai I, Gül A, Ohno S, Mizuki N. Association of major histocompatibility complex class I chain-related gene a and HLA-B alleles with Behçet's disease in Turkey. Jpn J Ophthalmol. 2007; 51(6):431–6. PMID: 18158593

17. Mizuki N, Ota M, Kimura M, Ohno S, Ando H, Katsuyama Y, et al. Triplet repeat polymorphism in the transmembrane region of the MICA gene: a strong association of six GCT repetitions with Behçet disease. Proc Natl Acad Sci U S A. 1997; 94(4):1298–303. PMID: 9037047

18. Wallace GR, Verity DH, Delamaine LJ, Ohno S, Inoko H, Ota M, et al. MIC-A allele profiles and HLA class I associations in Behçet's disease. Immunogenetics. 1999; 49(7–8):613–7. PMID: 10369918

19. Yasuoka H, Okazaki Y, Kawakami Y, Hirakata M, Inoko H, Ikeda Y, et al. Autoreactive CD8+ cytotoxic T lymphocytes to major histocompatibility complex class I chain–related gene A in patients with Behçet's disease. Arthritis Rheum. 2004; 50(11):3658–62. PMID: 15529349

20. Lehner T. Immunopathogenesis of Behçet's disease. Ann Med Interne (Paris). 1999; 150(6):483–7.

21. Baharav E, Weinberger A. The HLA-B*5101 molecule-binding capacity to antigens used in animal models of Behcet's disease: A bioinformatics study. Isr Med Assoc J. 2012; 14(7):424–8. PMID: 22953618

22. Alvarez-Márquez A, Aguilera I, Gentil MA, Caro JL, Bernal G, Alonso JF, et al. Donor-specific antibodies against HLA, MICA, and GSTT1 in patients with allograft rejection and C4d deposition in renal biopsies. Transplantation. 2009; 87(1):94–9. doi: 10.1097/TP.0b013e31818bd790 PMID: 19136897

23. Terasaki PI, Ozawa M, Castro R. Four-year follow-up of a prospective trial of HLA and MICA antibodies on kidney graft survival. Am J Transplant. 2007; 7(2):408–15. PMID: 17229080

24. Suárez-Alvarez B, López-Vázquez A, Díaz-Peña R, Díaz-Molina B, Blanco-García RM, Alvarez-López MR, et al. Post-transplant soluble MICA and MICA antibodies predict subsequent heart graft outcome. Trans Immunol. 2006; 17(1):43–6.

25. Link J, Kockum I, Lorentzen AR, Lie BA, Celius EG. Importance of human leukocyte antigen (HLA) class I and II alleles on the risk of multiple sclerosis. PLoS ONE. 2012; 7(5):e36779. doi: 10.1371/journal.pone.0036779 PMID: 22586495

26. Benacerraf B, McDevitt HO. Histocompatibility linked immune response genes. Science. 1972; 175:273–9. PMID: 4109878

27. Parham P, Lomen CE, Lawlor DA, Ways JP, Holmes N, Coppin HL, et al. Nature of polymorphism in HLA-A,-B, and-C molecules. Proc Natl Acad Sci USA. 1988; 85:4005–9. PMID: 3375250

28. Townsend A, Bodmer H. Antigen recognition by class I-restricted T lymphocytes. Annu Rev Immunol. 1989; 7:601–24. PMID: 2469442

29. Rudolph MG, Stanfield RL, Wilson IA. How TCRs bind MHCs, peptides, and coreceptors. Annu Rev Immunol. 2006; 24:419–66. PMID: 16551255

30. Holland CJ, Cole DK, Godkin A. Re-directing CD4(+) T cell responses with the flanking residues of MHC class II-bound peptides: The core is not enough. Front Immunol. 2013; 4(172):1–9.

31. Macdonald IK, Harkiolaki M, Hunt L, Connelley T, Carroll AV. MHC class I bound to an immunodominant *Theileria parva* epitope demonstrates unconventional presentation to T cell receptors. PLoS Pathog. 2010; 6(10):e1001149. doi: 10.1371/journal.ppat.1001149 PMID: 20976198

32. Mizuki N, Ohno S, Ando H, Chen L, Palimeris GD, Stavropoulos-Ghiokas E, et al. A strong association between HLA-B*5101 and Behçet's disease in Greek patients. Tissue Antigens. 1997; 50(1):57–60. PMID: 9243757

33. Itoh Y, Inoko H, Kulski JK, Sasaki S, Meguro A, Takiyama N, et al. Four-digit allele genotyping of the HLA-A and HLA-B genes in Japanese patients with Behcet's disease by a PCR-SSOP-Luminex method. Tissue Antigens. 2006; 67(5):390–4. PMID: 16671946

34. Chung YM, Yeh TS, Sheu MM, Chen MS, Wen MS, Tsai HY, et al. Behcet's disease with ocular involvement in Taiwan: a joint survey of six major ophthalmological departments. J Formos Med Assoc. 1990; 89(5):413–7. PMID: 1977855

35. Kurata R, Yonezawa T, Inoko H. Association analysis of the polymorphism of human leukocyte antigen-A,-B and-E gene with Behcet's disease in Japanese cohort using sequencing-based typing method. MOJ Immunol. 2014; 1(3):00013.

36. Kaburaki T, Takamoto M, Numaga J, Kawashima H, Araie M, Ohnogi Y, et al. Genetic association of HLA-A*2601 with ocular Behçet's disease in Japanese patients. Clin Exp Rheumatol. 2010; 4 Suppl 60:S39–44.

37. Kang EH, Kim JY, Takeuchi F, Kim JW, Shin K, Lee EY, et al. Associations between the HLA-A polymorphism and the clinical manifestations of Behcet's disease. Arthritis Res Ther. 2011; 13(2):R49. doi: 10.1186/ar3292 PMID: 21429233

38. Maenaka K, Maenaka T, Tomiyama H, Takiguchi M, Stuart DI, Jones EY. Nonstandard peptide binding revealed by crystal structures of HLA-B*5101 complexed with HIV immunodominant epitopes. J Immunol. 2000; 165(16):3260–7.

39. Blicher T, Kastrup JS, Buus S, Gajhede M. High-resolution structure of HLA-A*1101 in complex with SARS nucleocapsid peptide. Acta Crystallogr D Biol Crystallogr. 2005; 61(Pt 8):1031–40. PMID: 16041067

40. Menssen R, Orth P, Ziegler A, Saenger W. Decamer-like conformation of a nona-peptide bound to HLA-B*3501 due to non-standard positioning of the C terminus. J Mol Biol. 1999; 285(2):645–53. PMID: 9878435

41. Madrigal JA, Hildebrand WH, M. P. Belich MP, Benjamin RJ, Little AM, Zemmour J, et al. Structural diversity in the HLA-A10 family of alleles: correlations with serology. Tissue Antigens. 1993; 41(2):72–80. PMID: 8475492

42. Case DA, Darden TA, Cheatham TEI, Simmerling CL, Wang J, Duke RE, et al. AMBER10. University of California: San Francisco2008.

43. Duan Y, Wu C, Chowdhury S, Lee MC, Xiong G, Zhang W, et al. A point-charge force field for molecular mechanics simulations of proteins based on condensed-phase quantum mechanical calculations. J Comput Chem. 2003; 24(16):1999–2012. PMID: 14531054

44. Olsson MH, Søndergaard CR, Rostkowski M, Jensen JH. PROPKA3: consistent treatment of internal and surface residues in empirical pKa predictions. J Chem Theory Comput. 2011; 2:525–37.

45. Guillot B. A reappraisal of what we have learnt during three decades of computer simulations on water. J Mol Liq. 2002; 101(1–3):219–60.

46. Berendsen HJC, Postma JPM, Gunsteren WFv, DiNola A, Haak JR. Molecular dynamics with coupling to an external bath. J Chem Phys. 1984; 81:3684–90.

47. Ryckaert JP, Ciccotti G, Berendsen HJC. Numerical integration of Cartesian equations of motion of system with constraints: molecular dynamics of n-alkanes. J Comput Phys. 1997; 23(3):327–41.

48. Darden T, York D, Pedersen L. Particle mesh Ewald: An N·log(N) method for Ewald sums in large systems. J Chem Phys. 1993; 98(10089):10089–92.

49. Ren P, Ponder JW. Consistent treatment of inter- and intramolecular polarization in molecular mechanics calculations. J Comput Chem. 2002; 23:1497–506. PMID: 12395419

50. Decha P, Rungrotmongkol T, Intharathep P, Malaisree M, Aruksakunwong O, Laohpongspaisan C, et al. Source of high pathogenicity of an avian influenza virus H5N1: why H5 is better cleaved by furin. Biophys J. 2008; 95(1):128–3. doi: 10.1529/biophysj.107.127456 PMID: 18375507

51. Nunthaboot N, Rungrotmongkol T, Malaisree M, Kaiyawet N, Decha P, Sompornpisut P, et al. Evolution of human receptor binding affinity of H1N1 hemagglutinins from 1918 to 2009 pandemic influenza A virus. J Chem Inf Model. 2010; 50(8):1410–7. doi: 10.1021/ci100038g PMID: 20726599

52. Rungrotmongkol T, Nunthaboot N, Malaisree M, Kaiyawet N, Yotmanee P, Meeprasert A, et al. Molecular insight into the specific binding of ADP-ribose to the nsP3macro domains of chikungunya and venezuelan equine encephalitis viruses: Molecular dynamics simulations and free energy calculations. J Mol Graphics Modell. 2010; 29:347–53.

53. Wang Q, Pang YP. Normal-mode-analysis-monitored energy minimization procedure for generating small-molecule bound conformations. PLoS One. 2007; 2(10):e1025. PMID: 17925873